Pergamon

Int. Comm. Heat Mass Transfer, Vol. 29, No. 6, pp. 841-851, 2002

0735–1933/02/$–see front matter

PII: S0735-1933(02)00374-3

FLOW AND HEAT TRANSFER MEASUREMENTS IN LAMINAR AND TURBULENT CONVEX SURFACE BOUNDARY LAYERS

A.A. Ozalp and H. Umur
Mechanical Engineering Department,
Uludag University, 16059, Bursa, Turkey

(Communicated by J.P. Hartnett and W.J. Minkowycz)

ABSTRACT

Convex surface boundary layers have been experimentally investigated in a low speed wind tunnel, in the presence of pressure gradients (k) of $-3.6\text{x}10^{-6} \leq k \leq +3.6\text{x}10^{-6}$ for laminar and $-0.6\text{x}10^{-6} \leq k \leq +0.6\text{x}10^{-6}$ for turbulent flows. Flow and heat transfer measurements showed that stabilising effects of favourable pressure gradients caused thinner boundary layers, fuller velocity profiles and corresponding higher heat transfer rates. Downstream laminar and turbulent heat transfer measurements were below the flat plate laminar analytical solution and turbulent correlation by 54.2% and 25% respectively. It was also found that turbulent flow caused a heat transfer augmentation of 56.1% above the laminar values. Streamwise heat transfer variations, both in laminar and turbulent flows, appeared to be more affected by Reynolds number (Re_x) than streamwise pressure gradient (k_x). The mild pressure gradient of $k=2.0\text{x}10^{-6}$ increased the laminar heat transfer rates by 10.4%, whereas similar augmentation (11.8%) were recorded at $k=0.4\text{x}10^{-6}$ for turbulent flow, showing the significance of pressure gradients in turbulent flows. Furthermore by the new empirical equations, experimental flow and heat transfer parameters can be estimated with a precision of better than 6.8%. **© 2002 Elsevier Science Ltd**

Introduction

In many industrial applications, like turbine blades, aircraft wings and cooling fins, convex surfaces constitute a great importance both from fluid mechanics and heat transfer point of view. The flow type over convex surfaces, being laminar or turbulent, together with the streamwise location, thus the Reynolds number (Re_x), come out to be the primary headlines and starting points of experimental studies but in many cases flow acceleration or deceleration, due to pressure gradients ($k=(\nu/U^2)(dU/dx)$), are of great importance.

Several previous investigations exist on boundary layer development of convex surfaces. Laminar and turbulent flow measurements were performed by Plesniak et al. [1], who showed that the spanwise variations in the mean velocity and Reynolds stresses are due to streamwise vorticity. Turner et al. [2]

worked on a 1200 mm curvature and put forward that a mild favourable pressure gradient caused heat transfer values to increase by 13% and 8% in the laminar and turbulent flows respectively and moreover reported the gap between the turbulent and laminar heat transfer rates as 75%. Wang and Simon [3] also worked on the transitional boundary layers and reported the transition delaying role of convex curvature with 5% to 10% decrease of heat transfer in the late-transitional and early turbulent regions. Webster et al. [4] reported that the friction factor appeared to be most influenced by the decelerating turbulent flows over convex curvatures and measured thinner boundary layer in the presence of a favourable pressure gradient. Skin friction measurements, in the presence of adverse pressure gradient, were performed by Flittie and Covert [5], who reported reduced values with higher angle of attack. Muck et al. [6] investigated the effect of convex curvature on turbulent flows and concluded that the response of turbulence to convex curvature is rather rapid, without large changes in eddy viscosity distribution. Abuaf and Kercher [7] measured high heat transfer rates at the trailing edge of a turbine blade, where Re_x is low but turbulence intensities are above 50%.

This work covers the flow and heat transfer measurements, in laminar and turbulent convex surface boundary layers, in the presence and adverse and favourable pressure gradients. Since the aim is to investigate both the development of convex surface boundary layers and the effects of Re_x and k on flow and heat transfer parameters, measurements are not only presented, as to form a detailed overview, together with analytical solutions-correlations but also with respect to streamwise pressure gradient (k_x), from –0.47 to +0.47, encompassing the laminar and turbulent flows.

Flow Conditions and Instrumentation

All experiments were carried out in an open, low speed wind tunnel, run by a 5.7 kW axial blower. As shown in Figure 1(a), before entering the test section, air was drawn in through a screen pack, a nozzle and a straightening duct. The screen pack, composed of 7 rows of gause wire screen with a cross-sectional area of 2x2 mm^2, was used to obtain smooth streamlines, together with the 400 mm and 2:1 contraction nozzle, which was placed after the screen pack. An additional 400 mm duct was assembled to the upstream of the test section, after the nozzle, to eliminate the contraction effects. The 1000 mm in length transparent plexiglass experimental setup, designed and constructed in the Mechanical Engineering Department of Uludag University, has an initial test section area of 200x305 mm^2. The test surface, with a heated surface area (A) of 1000x240 mm^2, is a copper convex wall, 1500 mm in radius. As flowrates were adjusted by a butterfly valve, a false roof, hinged at the inlet, was capable of generating laminar and turbulent streamwise pressure gradients of $-3.6\times10^{-6}\leq k\leq+3.6\times10^{-6}$ and $-0.6\times10^{-6}\leq k\leq+0.6\times10^{-6}$ respectively, with an accuracy of ±5%. Uniform heat flux condition is generated on the flow surface by fixing the silicon coated 0.1 mm in diameter chrome-nickel resistive wire knitting on the backside of the copper plate, with an insulating layer beneath to minimise heat conduction loss, as shown in Figure 1(b). Streamwise and pitchwise velocity profile measurements were carried out using static pressure tabs, having a diameter of 1 mm, in conjunction with a semi square edged pitot tube and pressures were recorded by a micro manometer with a precision of ±1%. Static pressure tappings, first located 60 mm from the leading edge, were separated by 120 mm from each other in the streamwise direction, assuming the spanwise variation of static pressure to be constant and the movement of the pitot tube was oriented by a traverse mechanism having an accuracy of 0.5 mm. As the wall and flow temperatures were recorded by copper-constantan thermocouples, the heat flux on the convex copper wall was regulated with a variable AC voltage controller, capable of generating iso-temperature distribution, within ±0.5 °C, at no-flow condition. Convection heat loss (W/m^2) was estimated from the difference between the flow-on ($q_F=V_FI_F/A$) and flow–off ($q_o=V_oI_o/A$) powers required to maintain the same wall temperature at the 1st station with and without flow, where V and I are the voltage and current values of Figure 1(b). Using these power values, heat transfer coefficient and the corresponding Stanton number are calculated as $h=(q_F-q_o)/(T_w-T_o)$ and $St=h/\rho UC_p$ respectively. The uncertainties involved in the velocity and heat transfer measurements were 3% and 5% respectively and translated into the results as defined by Umur et al. [8].

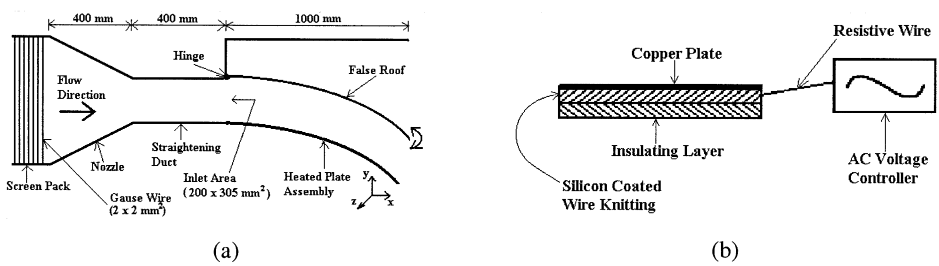

FIG. 1.
(a) Experimental setup and (b) heated plate assembly.

Experiments were performed in the range of $2.8x10^5 \leq Re_x \leq 4x10^5$ and $5.3x10^6 \leq Re_x \leq 5.9x10^6$ for free stream velocities of 3 m/s and 15 m/s respectively, which cover the laminar and turbulent regions. The initial station, 60 mm downstream of the inlet, boundary layer thickness δ was 14 mm and 12 mm, the corresponding initial values of Re_θ and H were 360-1550 and 2.92-1.71 for laminar and turbulent flows.

Results and Discussion

Experiments were performed at inlet core velocities of 3 m/s and 15 m/s, which form laminar and turbulent flows respectively and measurements were carried out at 6 stations of x=60, 180, 300, 420, 540 and 660 mm downstream of the inlet. As the pressure gradients of the laminar and turbulent flows were k=0, ±2.0 and $\pm 3.6x10^{-6}$ and k=0, ±0.4 and $\pm 0.6x10^{-6}$, effects of Re_x and k are discussed through the variations of velocity profiles, static pressures, shape factor (H), momentum thickness Reynolds number (Re_θ) and Stanton number (St) both in the streamwise direction and with respect to the streamwise pressure gradient of $k_x=kRe_{xp}$, where $Re_{xp}=Ux_p/\nu$ and x_p is the pressure gradient imposed length. Although laminar and turbulent flow regimes are handled under separate sub-headings, comparisons in between, together with the literature and analytical solutions, are procured whenever necessary.

Laminar Flow

Free stream inlet velocity of 3 m/s formed an initial station boundary layer thickness (δ) of 14 mm at x=60 mm, that corresponds to an unheated starting length (x_l) of 1430 mm, which is calculated by Blasius' analytical method [9] of $\delta=5x/Re_x^{0.5}$, thus an inlet Re_x of $2.8x10^5$. First station velocity profiles are not affected by the pressure gradients (Figure 2(a)), but the deviations become apparent beginning with the 2nd station (x=180 mm, $Re_x=3.1x10^5$).

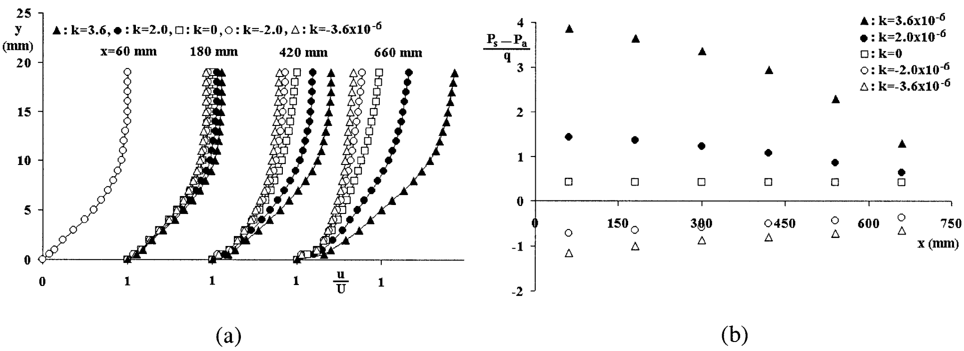

FIG. 2
Variation of (a) velocity profiles and (b) static pressures in laminar flow.

Accelerating flows of k=2, $3.6x10^{-6}$ produced an increase in $U_{x=660\ mm}$ by 35% and 91% and resulted in 4.5% and 9.2% thinner $\delta_{x=660\ mm}$. On the other hand, adverse pressure gradients of k=-2, $-3.6x10^{-6}$ constituted the contrary with the deceleration rates of 21% and 31% and thicker $\delta_{x=660\ mm}$ by 4% and 7.6%. Stabilising effects of favourable gradients, together with the deviations of accelerating patterns from the near zero gradient profiles, appear upstream of the destabilising role of the adverse gradients. Moreover velocity profiles at the downstream of the 5th station (x=540 mm, $Re_x=3.7x10^5$) for $k=-3.6x10^{-6}$ are similar to Muck et al.'s [6] transitional measurements. As the thinner δ of favourable gradient cases are accompanied with the fuller velocity profiles, thus higher skin friction coefficients (C_f), adverse gradient recordings show no sign of separation in spite of the convex curvature. Static pressure variations, given in Figure 2(b), imply positive and negative values for accelerating and decelerating flows respectively, but towards downstream all measurements converge to manometric zero, being the atmospheric pressure. Inlet static pressures at $k=2x10^{-6}$ and $k=-3.6x10^{-6}$ are close, with opposite signs, which verifies the similar acceleration and deceleration rates at these conditions, on the other hand the highest acceleration rate of $k=3.6x10^{-6}$ caused the most augmented non-dimensional static pressure at the inlet with the value of 3.87.

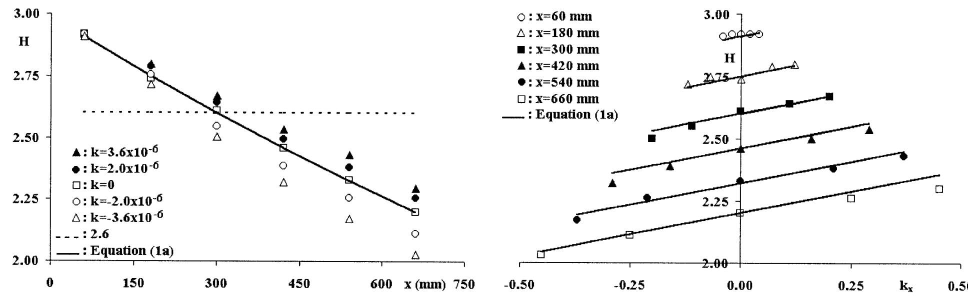

(a) (b)

FIG. 3
Variation of H (a) in streamwise direction and (b) with respect to k_x in laminar flow.

As for the velocity profiles, 1st station H data coincide with the value of 2.92 (Figure 3(a)), which is above the laminar characteristic value of 2.6 for the flat surface flows and 2.6 is attained at the 3rd station (x=300 mm, $Re_x=3.3x10^5$) in the streamwise direction. Excluding the case for $k=-3.6x10^{-6}$, all H records are in and above laminar findings of Plesniak et al. [1]. Decrease of H in the flow direction is common for with and without pressure gradient flows. Due to the stabilising role of accelerating flows, last station H are above that of the k=0 case, however lower recordings for the decelerating flows imply the shift towards transition, which strengthens the discussions through the velocity profiles of $k=-3.6x10^{-6}$ flow. The last station (x=660 mm, $Re_x=4x10^5$) H value for $k=-3.6x10^{-6}$ is slightly above Flittie and Covert's [5] turbulent values, thus together with the velocity profiles this can be considered as a sign of transition. It can be said that, from the point of transition onset, velocity profiles and H values are in good harmony. Combined effects of Re_x and k on H are demonstrated in Figure 3(b), showing the increase in H with $+k_x$ and the contrary with $-k_x$. Furthermore through Figures 3(a)-(b), Equation (1a) is derived, which can estimate experimental H values with maximum and average errors of 2.5% and 0.6% respectively.

$$H_{lam} = 5.84\exp\left(-2.45x10^{-6}Re_x\right) + 0.35k_x \qquad Re_{\theta,lam} = 124\exp\left(3.77x10^{-6}Re_x\right) - 44k_x \qquad \text{(1a-b)}$$

Streamwise variations of Re_θ and streamwise pressure gradient effects are shown in Figure 4(a), together with the Blasius' laminar analytic flat plate solution [9] of $\theta=0.664(\nu x/U)^{0.5}$. Streamwise increase in Re_θ can be observed through Figure 4(a); as the initial station data are projecting on each other with the value of 360, at the downstream section (x=660 mm, $Re_x=4x10^5$) they become 538, 559 and 580 for the flows with k=3.6, 0, -3.6x10^{-6} respectively. These findings are clearly above the flat plate values, below Muck et al.'s [6] and Flittie and Covert's [5] turbulent establishments and in good harmony with Plesniak et al.'s [1] laminar measurements. However among the last station (x=660 mm, Re_x=4x10^5) data, that of k=-3.6x10^{-6} is above the laminar but below the turbulent limits of Plesniak et al. [1], which can be accounted for a mark of transition, being in conjunction with velocity profile and H discussions. As in the H investigations, effects of Re_x and k are disclosed by the supplementary plot of Figure 4(b). Contrary to the H variation, Re_θ decreases with $+k_x$ and increases with $-k_x$ and this relation is characterised by the presented formula of Equation (1b), which evaluates experimental values with maximum and average errors of 1.6% and 0.6% respectively.

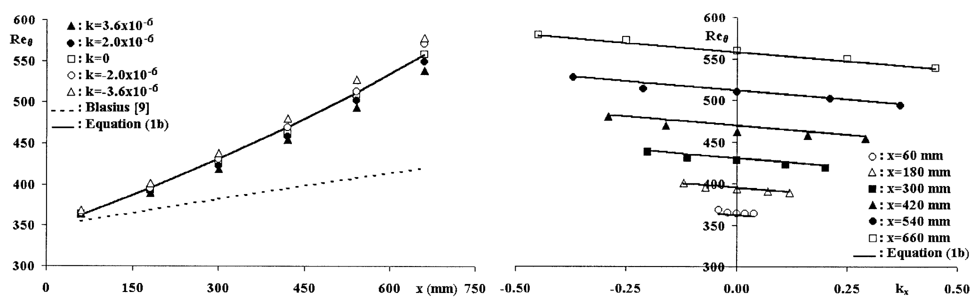

(a) (b)

FIG. 4
Variation of Re_θ (a) in streamwise direction and (b) with respect to k_x in laminar flow.

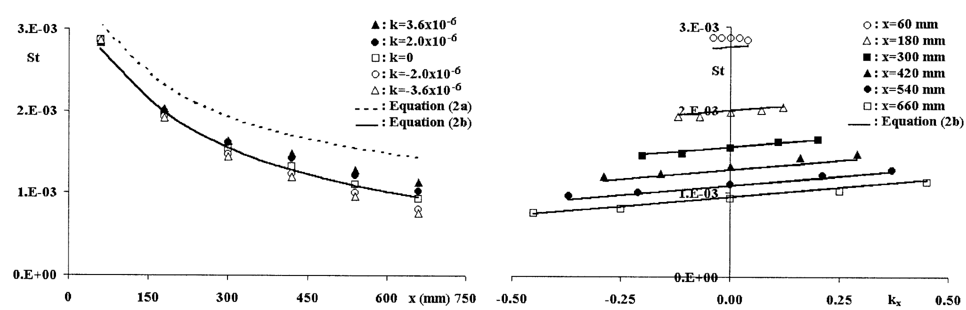

(a) (b)

FIG. 5
Variation of St (a) in streamwise direction and (b) with respect to k_x in laminar flow.

Results of the synchronised heat transfer measurements have shown that, under constant heat flux condition, convex surface St values are below the flat plate laminar analytical solution of Equation (2a), where Pr is the Prandtl number. As the deviation is 6.3% at the 1st station (x=60 mm, Re_x=2.8x10^5), towards the end of the test section (x=660 mm, $Re_x=4x10^5$) it expands to 54.2%. The initial station data of Figure 5(a) are identical, verifying the flow measurements, and streamwise decay of heat transfer values are observed for all cases. Results showed that favourable gradients increased St in the flow direction, which can be attributed to the thinner δ and higher C_f of accelerating flows. However the reverse effects are determined for the flows with adverse pressure gradients, which form thicker δ due to destabilising role. St values of k=0 case are lower than Turner et al.'s [2] laminar reports for 1200 mm curvature and can be explained through Wang and Simon's [3] findings regarding the higher heat transfer rates with strong convex curvature. Moreover Turner et al. [2] informed an augmentation in St by 13% in the presence of mild favourable gradient, which is in agreement with the present results of 10.4% St increase for the laminar flow with $k=2.0x10^{-6}$. On the other hand decrease rates in St, due to deceleration, are lower than the augmentation in acceleration, implying that the influence of favourable gradients is more than the adverse, which also agrees with the velocity measurements.

$$St = 0.453Re_x^{-0.5}Pr^{-2/3}\left[1-\left(\frac{x_1}{x}\right)^{0.75}\right]^{-1/3} \qquad St_{lam} = 0.64Re_x^{-0.5}\left[1.6-\left(\frac{x_1}{x}\right)^{1.5}\right]^{-2} + 4.6x10^{-4}k_x \quad \text{(2a-b)}$$

Moreover, Figure 5(b) shows that, by the new empirical formula of Equation (2b) experimental St, for laminar convex surface flows, can be estimated with maximum and average errors of 4.9% and 2.5%. This equation puts forward that the effect of Re_x on St variation is more influential than k, since as the strongest favourable gradient of $k=3.6x10^{-6}$ increases the downstream heat transfer by 22%, the ratio of the 3rd (x=300 mm, $Re_x=3.3x10^5$) and 6th (x=660 mm, $Re_x=4x10^5$) station St values, for k=0 flow, is 66%.

Turbulent Flow

The boundary layer thickness of the 1st station, for the free stream inlet velocity of 15 m/s, was measured as 12 mm, being thinner than the corresponding data for the laminar flow with U=3 m/s and is an initial sign of turbulent character at $Re_x=5.3x10^6$. Pressure gradients are not effective on the first station velocity profiles (Figure 6(a)), but with the 2nd station (x=180 mm, $Re_x=5.4x10^6$) variations arise. As the last station (x=660 mm, $Re_x=1x10^6$) δ decreased by 9.5% and 15.2% at k=0.4, $0.6x10^{-6}$, with an increase in $U_{x=660\ mm}$ by 37% and 68%, adverse pressure gradients of k=-0.4, $-0.6x10^{-6}$ produced deceleration rates of 20% and 27% and thicker $\delta_{x=660\ mm}$ by 8.8% and 14.1%. The velocity profiles, of the near zero and adverse pressure gradient flows, are similar to Webster et al.'s [4] turbulent measurements; on the other hand velocity profiles of the last 2 stations ($Re_x \geq 5.73x10^6$) at $k=0.6x10^{-6}$ resemble Muck et al.'s [6] transitional findings, which can be connected to the stabilising effects of favourable gradients. Static pressure variations, given in Figure 6(b), are in conjunction with the laminar case, with the positive manometric pressures for accelerating flows and with the reverse for the deceleration cases. Inlet static pressure of k=0.4x10^{-6} is more than that of k=-0.6x10^{-6}, verifying the above comparison on streamwise flow velocity variation. On the other hand, the highest acceleration rate of k=0.6x10^{-6} caused the highest non-dimensional static pressure at the inlet with the value of 2.29.

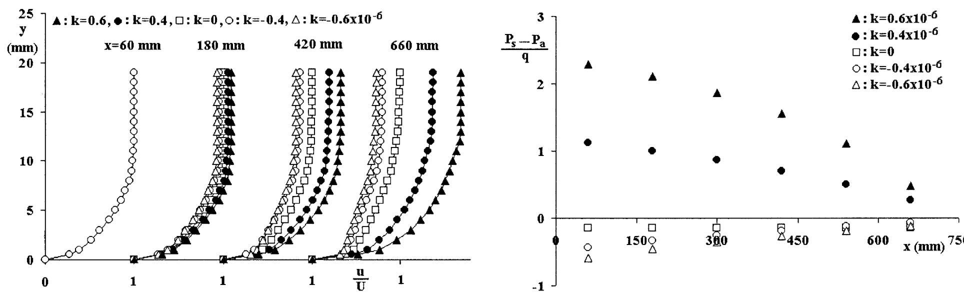

(a) (b)

FIG. 6
Variation of (a) velocity profiles and (b) static pressures in turbulent flow.

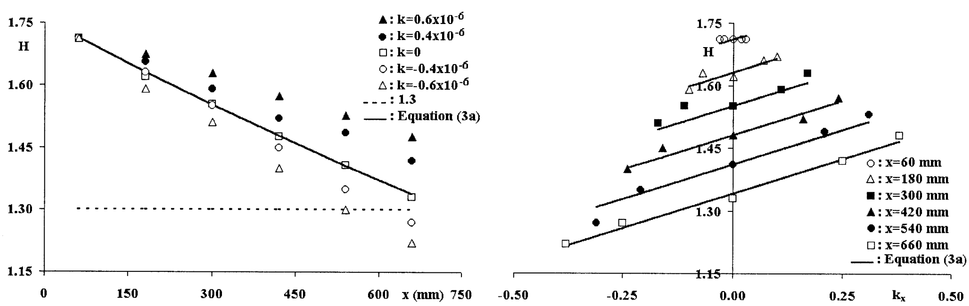

(a) (b)

FIG. 7
Variation of H (a) in streamwise direction and (b) with respect to k_x in turbulent flow.

The initial station H values (1.71) are significantly lower than the last station value (2.20) for U=3 m/s at k=0. As the characteristic value of 1.3, for turbulent flat surface flows, is not reached at k=0 case, the findings of near zero and adverse pressure gradient flows are outside Plesniak et al.'s [1] laminar data but inside Muck et al.'s [6] and Webster et al.'s [4] turbulent measurements. Streamwise decrease in H are also recorded at U=15 m/s for all cases (Figure 7(a)), together with the higher values with accelerating and lower values with decelerating flows. Although augmented H values for k=0.6x10^{-6} case, together with the velocity profiles imply a shift towards transition, the records are still close to Flittie and Covert's [5] turbulent findings, resembling the end of transition. These determinations are in conjunction with the findings through velocity profiles and point out the turbulent character, except for the downstream section of the flow with $k=0.6x10^{-6}$. Furthermore, as in the laminar flow, combined effects of Re_x and k on H are given in Figure 7(b). Equation (3a) establishes the influence of Re_x and k_x on H variation with maximum and average errors of 3% and 0.75%. It should also be noted that, the effects of k_x on H, both in the laminar and turbulent regions, are very close, since the constants defining the slopes in Figures 3(b)-7(b) are 0.35 and 0.33 for the Equations (1a)-(3a).

$$H_{turb} = 16.5\exp\left(-4.3x10^{-7}Re_x\right) + 0.33k_x \qquad Re_{\theta,turb} = 190\exp\left(4x10^{-7}Re_x\right) - 450k_x \qquad \text{(3a-b)}$$

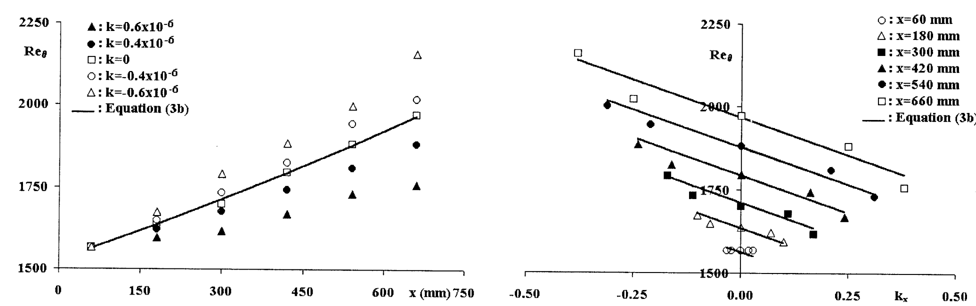

(a) (b)

FIG. 8
Variation of Re_θ (a) in streamwise direction and (b) with respect to k_x in turbulent flow.

As shown in Figure 8(a), turbulent Re_θ coincide at the initial station, with the value of 1550, which is particularly higher than the downstream data (559) of the laminar flow. As in the laminar case, accelerating flows produced lower Re_θ than the adverse and near zero gradient flows, moreover Re_θ kept on increasing in the streamwise direction. The last station (x=660 mm, $Re_x=5.9x10^6$) values are 1755, 1970 and 2159 for the flows with k=0.6, 0, $-0.6x10^{-6}$ respectively and they are within Flittie and Covert's [5] turbulent data. Moreover the results of the turbulent flat plate analytical solution of $\theta=0.036x/Re_x^{0.2}$ [9] proposes a Re_θ range of 8500-9300, which is far above the present values. Although the values are below Webster et al.'s [4] turbulent findings, flows with U=15 m/s can be said, from the point of Re_θ, fully turbulent, together with the strongest favourable gradient of $k=0.6x10^{-6}$. Variation of Re_θ with k_x is plotted in Figure 8(b), showing similar trends with the laminar case but the proposed empirical relation of Equation (3b), with maximum and average estimation errors of 2.9% and 0.95%, implies the more influential role of k_x, with the constant of 450, in the turbulent flow than the laminar case, where the similar constant is determined as 44 in Equation (1b).

Streamwise decay, increase with favourable gradients and decrease with adverse gradients are the common points of turbulent heat transfer results with that of the laminar. As the initial station experimental St of Figure 9(a) are higher than the flat plate turbulent correlation (Equation (4a)) and flat plate analytical solution (Equation (2a)) by 14.8% and 23%, at the 6th station (x=660 mm, $Re_x=5.9x10^6$) experimental St for k=0 is lower than the turbulent correlation by 20.3% and higher than analytical solution by 28.7%. Turbulent St values are above the laminar values of Figure 5(a) at the 1st and 6th stations by 30.3% and 97.9% and the streamwise average being 56.1%. Turner et al.'s [2] similar ratio is 75% and the difference can be explained with their strong curvature of 1200 mm and Ligrani and Hedlung [10] reported the proportion of the turbulent to transition St as 15.6% over a 596.9 mm curvature. On the other hand the mild gradient of $k=0.4x10^{-6}$ produced an increase in St by 11.8%, whereas the similar ratio of Turner et al. [2] is 8%, which is lower than that of the present work.

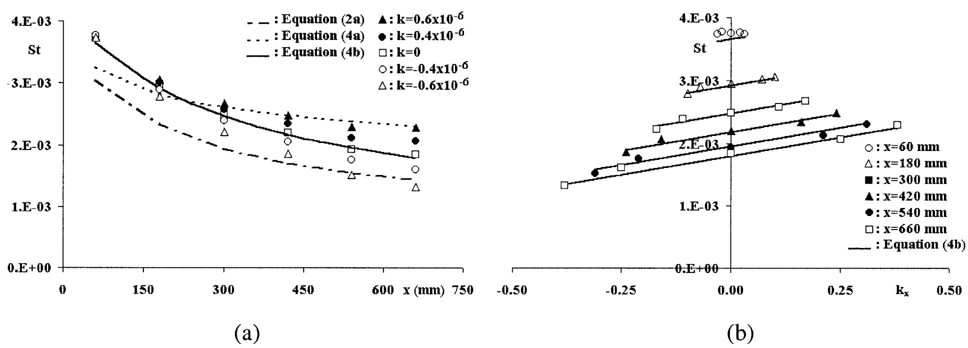

FIG. 9
Variation of St (a) in streamwise direction and (b) with respect to k_x in turbulent flow.

Moreover combined effects of Re_x and k on heat transfer rates can be seen in Figure 9(b), together with the present turbulent correlation (Equation (4b)), with maximum and average errors of 6.8% and 2.1% respectively. Like the laminar case, Re_x on turbulent heat transfer is superior to k; as the strongest favourable gradient of $k=0.6x10^{-6}$ increased the downstream heat transfer by 24%, the ratio of the 3rd ($x=300$ mm, $Re_x=5.5x10^6$) and 6th ($x=660$ mm, $Re_x=5.9x10^6$) station St values, for k=0 flow, is 35%.

$$St = 0.03 Re_x^{-0.2} Pr^{-0.4}\left[1-\left(\frac{x_1}{x}\right)^{0.9}\right]^{-1/3} \qquad St_{turb} = 0.036 Re_x^{-0.25}\left[1.1-\left(\frac{x_1}{x}\right)^{2}\right]^{-0.75} + 1.2x10^{-3} k_x \quad (4a\text{-}b)$$

Conclusion

Convex surface laminar and turbulent boundary layers, in the presence of favourable and adverse pressure gradients, have been experimentally investigated in terms of the flow and heat transfer characteristics. As favourable pressure gradients, both in laminar and turbulent flows, are determined to cause thinner boundary layers, fuller velocity profiles, higher C_f thus augmented heat transfer rates, results of the adverse pressure gradients are the contrary due to their destabilising role. Laminar and turbulent heat transfer measurements are below the flat plate laminar analytical solution and turbulent correlation, showing the stabilising character of convex curvature and moreover turbulent St values are determined to be 56.1% above that of the laminar case. Effect of streamwise pressure gradient (k_x) on turbulent and laminar H are designated to be close, whereas k_x particularly more affected the turbulent Re_θ and St variations than that of the laminar flow. Streamwise heat transfer variations, both in laminar and turbulent flows, appeared to be more affected by Re_x than k_x and by the new empirical equations, flow and heat transfer parameters of H, Re_θ and St can be estimated with a precision of better than 6.8%.

Nomenclature

C_p	constant pressure specific heat, J/kgK
H	shape factor
k	pressure gradient parameter
k_x	streamwise pressure gradient
P_s, P_a	static and atmospheric pressures, Pa
q	dynamic pressure, Pa
Re_x	streamwise distance Reynolds number
Re_θ	momentum thickness Reynolds number
St	Stanton number
T_o, T_w	free stream and wall temperatures, °C
U	mean velocity, free stream velocity, m/s
x, y	streamwise and pitch wise direction, mm

Greek Symbols

δ	boundary layer thickness, mm
ν	kinematic viscosity, m^2/s
ρ	density, kg/m^3
θ	momentum thickness, mm

References

1. M. W. Plesniak, R. D. Mehta and J. P. Johnston, *Journal of Fluid Mechanics* **270**, 1, (1994).
2. A. B. Turner, S. E. H. Walker and F. J. Bayley, *Int. J. Heat and Mass Transfer* **43**, 251, (2000).
3. T. Wang and T. W. Simon, *Journal of Turbomachinery* **109**, 443, (1987).
4. D. R. Webster, D. B. Degraaff and J. K. Eaton, *Journal of Fluid Mechanics* **323**, 1, (1996).
5. K. J. Flittie and E. E. Covert, *AIAA Journal* **30**, 2647, (1992).
6. K. C. Muck, P. H. Hoffman and P. Bradshaw, *Journal of Fluid Mechanics* **161**, 347, (1985).
7. N. Abuaf and D. M. Kercher, *Journal of Turbomachinery* **116**, 169, (1994).
8. H. Umur, R. I. Crane and J. H. Whitelaw, *IMechE Part C* **209**, 1, (1995).
9. H. Schlichting, *Boundary Layer Theory*, 7th ed., p. 817. McGraw Hill, New York, (1979).
10. P. M. Ligrani and C. R. Hedlung, *Int. J. Heat and Mass Transfer* **41**, 1739, (1998).

Received May 24, 2002